Fourier Transform Infrared Spectrum of the Secondary Quinone Electron Acceptor Q_B in Photosystem II†

Hiroyuki Suzuki,‡ Masa-aki Nagasaka,‡ Miwa Sugiura,§ and Takumi Noguchi*,‡

Institute of Materials Science, University of Tsukuba, Tsukuba, Ibaraki 305-8573, Japan, and Department of Plant Bioscience, School of Life and Environmental Sciences, Osaka Prefecture University, 1-1 Gakuen-cho, Sakai, Osaka 599-8531, Japan

Received June 28, 2005; Revised Manuscript Received July 24, 2005

ABSTRACT: Fourier transform infrared difference spectra upon single reduction of the secondary quinone electron acceptor Q_B in photosystem II (PSII), without a contribution from the electron donor-side signals, were obtained for the first time using Mn-depleted PSII core complexes of the thermophilic cyanobacterium *Thermosynechococcus elongatus*. The Q_B^-/Q_B difference spectrum exhibited a strong C•••O stretching band of the semiquinone anion at 1480 cm^{-1}, the frequency higher by 2 cm^{-1} than that of the corresponding band of Q_A^-, in agreement with the previous $S_2Q_B^-/S_1Q_B$ spectrum of the PSII membranes of spinach [Zhang, H., Fischer, G., and Wydrzynski, T. (1998) *Biochemistry 37,* 5511−5517]. Also, several peaks originating from the Fermi resonance of coupled His modes with its strongly H-bonded NH vibration were observed in the 2900−2600 cm^{-1} region, where the peak frequencies were higher by 7−24 cm^{-1} compared with those of the Q_A^-/Q_A spectrum. These frequency differences suggest that H-bond interactions of the CO groups, especially with a His side chain, are different between Q_B^- and Q_A^-. Furthermore, a prominent positive peak was observed at 1745 cm^{-1} in the C═O stretching region of COOH or ester groups in the Q_B^-/Q_B spectrum. The peak frequency was unaffected by D_2O substitution, indicating that this peak does not arise from a COOH group but probably from the 10a-ester C═O group of the pheophytin molecule adjacent to Q_B. The absence of protonation of carboxylic amino acids upon Q_B^- formation in contrast to the previous observation in the purple bacterium *Rhodobacter sphaeroides* suggests that the protonation mechanism of Q_B in PSII is different from that of bacterial reaction centers.

Photosystem II (PSII)[1] is a multimeric protein complex that functions as a water-quinone oxidoreductase and is located at the electron donor terminal of the photosynthetic electron transport chain in plants and cyanobacteria. Light illumination triggers charge separation in PSII; on the electron donor side, water is oxidized to molecular oxygen and protons, and on the electron acceptor side, the primary quinone electron acceptor Q_A and then the secondary quinone acceptor Q_B are reduced (*1*). The chemical identity of both Q_A and Q_B is PQ-9. They are symmetrically located with respect to the non-heme iron center as recently visualized in the X-ray crystallographic structure of the PSII complex (*2*). Despite their homology, however, the reaction and function of Q_B are totally different from those of Q_A. While Q_A is only singly reduced and transfers an electron to Q_B, Q_B can be doubly reduced and then protonated to become PQH_2, which is released from the protein and replaced with another PQ molecule (*1*, *3*, *4*). In addition, electron transfer from Q_A^- to Q_B is suppressed at 250−260 K (*5*, *6*), whereas Q_A^- can be formed even at very low temperatures. These differences between Q_B and Q_A must be achieved by (i) fine control of the redox potentials of PQ molecules at the Q_A and Q_B sites by interactions with proteins so that an electron is smoothly transferred from Q_A to Q_B, (ii) the presence of the proton transfer pathways from the stromal surface to Q_B in the PSII proteins (*1*, *3*, *4*, *7*), and (iii) significant structural changes upon formation of Q_B^- that requires sufficient protein flexibility around Q_B (*5*, *6*). However, molecular mechanisms of these factors for realizing the Q_B function in PSII are yet to be clarified.

To answer these questions about Q_B, information about the detailed structure and molecular interactions of a PQ molecule and its semiquione radical in the Q_B pocket, which are usually beyond the resolution of X-ray crystallography, and about the protein responses upon Q_B reduction is essential. One of the most powerful methods of obtaining such information is light-induced Fourier transform infrared (FTIR) difference spectroscopy that can directly detect chemical bonds and their changes upon photochemical reactions (*8*). Indeed, this method has been extensively applied to the studies of Q_B and Q_A in purple bacterial RC, which structurally and functionally resemble those in PSII. Rather symmetric weak H-bonds were observed in the two C═O groups in Q_B, while significant asymmetry was detected in the H-bond interactions of the C_1═O and C_4═O groups in Q_A (*9*−*11*). In addition, protonation of the

† This study was supported by a Grant-in-Aid for Scientific Research (17GS0314) from the Ministry of Education, Culture, Sports, Science and Technology of Japan and by Special Research Project "Nano-Science" at the University of Tsukuba.

* To whom correspondence should be addressed. Phone: +81-29-853-5126. Fax: +81-29-855-7440. E-mail: tnoguchi@ims.tsukuba.ac.jp.

‡ University of Tsukuba.

§ Osaka Prefecture University.

[1] Abbreviations: Chl, chlorophyll; DCMU, 3-(3,4-dichlorophenyl)-1,1-dimethylurea; FTIR, Fourier transform infrared; Mes, 2-(*N*-morpholino)ethanesulfonic acid; Pheo, pheophytin; PSII, photosystem II; PQ, plastoquinone; PQH_2, plastoquinol; Q_A, primary quinone electron acceptor; Q_B, secondary quinone electron acceptor; RC, reaction center(s).

10.1021/bi051237g CCC: $30.25
Published on Web 08/06/2005

carboxylate group of L-Glu212 upon Q_B^- formation, which is involved in the mechanism of proton transfer to Q_B (*12*), has been directly observed in *Rhodobacter sphaeroides* RC as the appearance of a COOH peak at 1728 cm^{-1} (*13*−*15*). Furthermore, recent FTIR studies by Breton and co-workers (*16*−*18*) showed that Q_B is bound to the proximal site, the binding site closer to Q_A in the two distinct binding sites proposed by X-ray crystal structures (*19*), implying the absence of large-scale displacement of the quinone molecule before Q_B reduction.

Despite the functional similarity of Q_B between bacterial RC and PSII, the mechanism of its reaction and regulation could be considerably different. The involvement of bicarbonate, which is a ligand of the non-heme iron in PSII but not in bacterial RC, in the Q_A^- to Q_B electron transfer as well as the proton transfer to Q_B has been proposed (*7*), and the loop region between the D and E helices of the D1 subunit that forms the Q_B binding site has an extended sequence not found in the bacterial L subunit. However, molecular-level analyses of the Q_B structures and reactions in PSII have been rather delayed as compared with those of bacterial RC. FTIR signals of Q_B in PSII were only detected in the PSII-enriched membranes of spinach by Zhang et al. (*20*) as an $S_2Q_B^-/S_1Q_B$ spectrum including signals from the oxygen-evolving center. In this spectrum, the strong C⋯O stretching band of Q_B^- was recognized at 1480 cm^{-1}, the position higher by 2 cm^{-1} than that of Q_A^-. Other signals of Q_B, however, were difficult to identify because of the severe overlap of donor-side signals. For detailed analyses of the molecular interactions of Q_B and the protein responses upon its reduction in PSII, measurement of an FTIR spectrum arising only from the Q_B site and its coupled structures in proteins, without any contributions from redox reactions of other cofactors, is urgent.

In this study, we report for the first time a Q_B^-/Q_B FTIR difference spectrum in the absence of donor-side signals using the Mn-depleted PSII core complexes of *Thermosynechococcus elongatus*. Our His-tagged PSII complexes of *T. elongatus* possess an intact Q_B site with quite high Q_B occupancy as shown by thermoluminescence measurements (*21*), and hence, an almost pure Q_B^-/Q_B spectrum without contributions of Q_A signals was obtained. By comparing this spectrum with the Q_A^-/Q_A spectrum, we detected differences in molecular interactions of PQ between the Q_A and Q_B sites. Furthermore, the spectrum was analyzed by D_2O substitution, and the proton transfer mechanism upon Q_B reduction was suggested to be different from that of bacterial RC.

MATERIALS AND METHODS

PSII core complexes of *T. elongatus*, in which the carboxyl terminus of the CP43 subunit was genetically His-tagged, were purified as previously described (*21*). Mn depletion was performed by NH_2OH treatment (10 mM) at room temperature (*21*). An aliquot (4 μL) of Mn-depleted PSII core complexes (∼4.5 mg of Chl/mL) in 10 mM Mes-NaOH (pH 6.0), 25 mM sucrose, 5 mM NaCl, and 0.06% *n*-dodecyl β-D-maltoside was further mixed with 1 μL of 5 mM sodium bicarbonate, 1 μL of 5 mM NH_2OH, and 1 μL of 10 mM potassium ferrocyanide. Here, NH_2OH works as an exogenous electron donor, ferrocyanide as a mediator to oxidize the reduced form of Q_B by a small amount of ferricyanide in the ferrocyanide−ferricyanide equilibrium, and bicarbonate as a ligand of the non-heme iron to keep its structure intact. The sample solution was then dried on a CaF_2 plate with a N_2 gas flow, and a hydrated PSII core film was formed under the humidity control using a 20% (v/v) glycerol/water solution as described previously (*22*). For Q_A^-/Q_A measurements, 6 μL of H_2O and 0.5 μL of a 1 mM DCMU/ethanol solution (final ethanol concentration of <4%) were further added to the sample solution before the sample was dried. H−D substitution was performed by drying the sample solution and subsequent resuspension in the same volume of D_2O. This procedure was repeated three times followed by incubation at 10 °C for 12 h. A deuterated film was then formed using a 20% glycerol$(OD)_3/D_2O$ solution in a manner similar to that of the hydrated film.

FTIR spectra were measured using a Bruker IFS-66/S spectrophotometer equipped with an MCT detector (InfraRed D316/8) at 4 cm^{-1} resolution. The sample temperature was adjusted to 10 °C by circulating cold water in a copper holder. A Q_B^-/Q_B difference spectrum was obtained by recording single-beam spectra for 100 s (200 scans) before and 10 s after a single flash from a Q-switched Nd:YAG laser (Quanta-Ray GCR-130, 532 nm, ∼7 ns fwhm). The 10 s interval after flash illumination was inserted to remove a minor contribution of the Q_A^- component with a slow relaxation time (a few seconds). Two spectra obtained using two different samples (400 scans in total) were averaged for the final data. Repeated measurement of Q_B^-/Q_B spectra using the same sample was avoided because NH_2OH gradually becomes ineffective during long dark relaxation (1 h), and hence, the spectra are contaminated with $Y_D^\bullet/Y_D$ signals. A Q_A^-/Q_A difference spectrum was obtained from scans (100 s) before and after single-flash illumination and by repeating the measurements five times with a dark interval of 30 min.

RESULTS AND DISCUSSION

Figure 1a shows an FTIR difference spectrum of the Mn-depleted PSII core complexes of *T. elongatus* upon single-flash illumination at 10 °C. Since the sample includes NH_2OH as an exogenous electron donor, the spectrum that was obtained should exhibit the structural changes upon one-electron reduction of the quinone electron acceptor, either Q_A or Q_B. The prominent feature of this spectrum was a strong positive peak at 1480 cm^{-1} accompanied by satellite bands at 1455, 1446, and 1432 cm^{-1}. Indeed, such a strong peak with medium subpeaks in the 1500−1400 cm^{-1} region is typical of the FTIR spectra of semiquinone anions, and these signals have been attributed to the C⋯O stretching vibrations coupled with C⋯C stretches (*11*, *23*). Other prominent signals in this spectrum are a sharp positive peak at 1745 cm^{-1} in the C═O stretching region of COOH or ester groups [1780−1700 cm^{-1} (*24*)], peaks at 1699, 1685, 1664, 1657, 1646, 1635, 1623, and 1612 cm^{-1} in the region of amide I [C═O stretches of backbone amides (*25*)] and the C═O stretches of neutral quinone (*11*, *23*), and peaks at 1579, 1562, 1554, 1545, and 1519 cm^{-1} in the amide II [NH bend + CN stretch of backbone amides (*25*)] region.

The spectrum of Figure 1a was compared with the Q_A^-/Q_A FTIR difference spectrum (Figure 1c), which was recorded in the presence of DCMU at 10 °C. This Q_A^-/Q_A

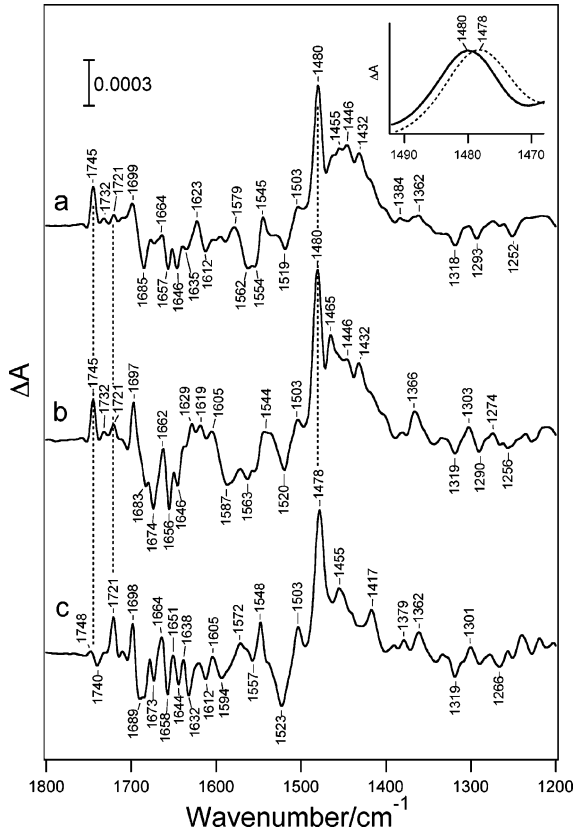

FIGURE 1: Flash-induced FTIR difference spectra (1800−1200 cm^{-1}) of the quinone electron acceptors in the Mn-depleted PSII core complexes of *T. elongatus*: (a) Q_B^-/Q_B difference spectrum in H_2O buffer, (b) Q_B^-/Q_B difference spectrum in D_2O buffer, and (c) Q_A^-/Q_A difference spectrum in H_2O buffer in the presence of DCMU. The inset is an expanded view of the strongest C⋯O stretching bands of the Q_B^-/Q_B (—) and Q_A^-/Q_A (- - -) spectra in H_2O buffer.

spectrum was basically identical to the previously reported one of the *T. elongatus* core complexes measured at −10 °C by Remy et al. (*26*). It is noted that the effect of DCMU binding on the Q_A^-/Q_A spectrum was negligible judging from the Q_A^-/Q_A spectra measured at 220 K with and without DCMU (not shown). Although overall features of the two spectra in panels a and c of Figure 1 are similar, the spectrum without DCMU (Figure 1a) exhibits several characteristics clearly different from those of the Q_A^-/Q_A spectrum (Figure 1c). (i) The frequency of the strong positive peak at 1480 cm^{-1} is higher by 2 cm^{-1} than that of the corresponding peak of Q_A^- at 1478 cm^{-1} (Figure 1, inset). Note that this 2 cm^{-1} difference was ensured by the FTIR measurements at 2 cm^{-1} resolution (data not shown). (ii) The broad feature by the overlap of several bands in the 1470−1400 cm^{-1} region (Figure 1a) is significantly different from the relatively sharp peaks at 1455 and 1417 cm^{-1} in the Q_A^-/Q_A spectrum (Figure 1c). (iii) In the COOH/ester C═O region, the sharp positive peak at 1745 cm^{-1} (Figure 1a) was absent and replaced with a weak differential signal at 1748/1740 cm^{-1} in the Q_A^-/Q_A spectrum (Figure 1c). Instead, a similar sharp positive peak was observed at 1721 cm^{-1} in Q_A^-/Q_A (Figure 1c). (iv) Negative peaks at 1673 and 1632 cm^{-1} in the amide I/quinone C═O region of the Q_A^-/Q_A spectrum lost the intensities exhibited by the spectrum in Figure 1a. (v) The relative intensities of the ∼1558, 1545, and 1519 cm^{-1} bands in the amide II region (Figure 1a) are significantly different

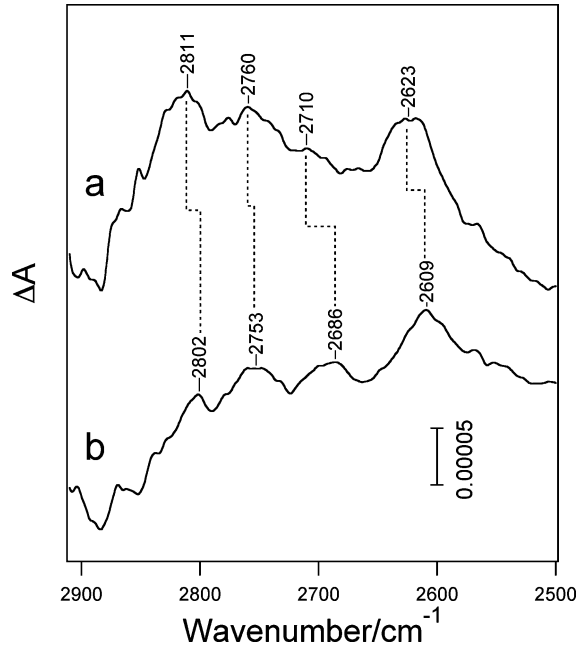

FIGURE 2: Q_B^-/Q_B (a) and Q_A^-/Q_A (b) difference spectra of the Mn-depleted PSII core complexes of *T. elongatus* in the 2900−2500 cm^{-1} region where Fermi resonance peaks of the coupled His appear.

from those of the 1556, 1548, and 1523 cm^{-1} bands in the Q_A^-/Q_A spectrum (Figure 1c).

These clear differences between the spectra in the absence (Figure 1a) and presence (Figure 1c, Q_A^-/Q_A) of DCMU indicate that the spectrum in Figure 1a represents a Q_B^-/Q_B difference spectrum. The only minor intensity at 1721 cm^{-1} (Figure 1a), where the typical Q_A^-/Q_A band appears (Figure 1c), suggests that this is an almost pure Q_B^-/Q_B spectrum.

The frequency of the strongest C⋯O peak of Q_B^- at 1480 cm^{-1} and the upshift by 2 cm^{-1} from that of Q_A^- are in good agreement with the previous observation in the $S_2Q_B^-/S_1Q_B$ spectrum of PSII-enriched membranes of spinach by Zhang et al. (*20*). Our measurement of a Q_B^-/Q_B spectrum using the Mn-depleted PSII membranes of spinach also showed the strong positive peak at 1480 cm^{-1} (not shown), although some contributions of Q_A^-/Q_A signals, which are probably ascribed to the unoccupied Q_B site in the fraction of centers, were evident judging from the presence of 1725/1719 cm^{-1} peaks typical of Q_A^-/Q_A of spinach PSII (*27*). Thus, the C⋯O frequency slightly higher than that of Q_A^- is a common feature of Q_B^- in PSII preparations regardless of species.

Figure 2 shows the Q_B^-/Q_B (a) and Q_A^-/Q_A (b) spectra of the PSII core complexes of *T. elongatus* in the higher-frequency region of 2900−2500 cm^{-1}. The several small peaks in this region of the Q_A^-/Q_A spectrum (Figure 2b) were previously assigned, by selective [^{15}N]His labeling of *Synechocystis*, to the Fermi resonance peaks of the overtones or combinations of His modes coupled to the NH vibration, which appear when the His NH group is engaged in a strong H-bond (*28*). The broad feature under these peaks may arise from the NH stretch of His itself or from polarizable protons in the H-bond network as proposed by Breton and Nabedryk (*29*) for the continuum bands in bacterial Q_A^-/Q_A and Q_B^-/Q_B spectra. The Q_B^-/Q_B spectrum of PSII also exhibited a similar feature of several peaks on a broad background

(Figure 2a). The peak positions, however, were clearly different from those of Q_A^-/Q_A. The frequencies at 2811, 2760, 2710, and 2623 cm^{-1} in Q_B^-/Q_B were higher by 9−24 cm^{-1} than those at 2802, 2753, 2686, and 2609 cm^{-1}, respectively, in Q_A^-/Q_A. Note that identification of other His bands below 1800 cm^{-1}, including the C−N stretch around 1100 cm^{-1} (not shown), needs to be studied further by isotopic labeling of His because of severe overlap of quinone and protein bands (*28*).

The observations of the similar Fermi resonance peaks of His described above suggest that there are homologous His−PQ interactions in the Q_A and Q_B sites. These His residues are most probably D2-His214 and D1-His215, which connect Q_A and Q_B, respectively, with the non-heme Fe^{2+} (*2*). Despite the homology in the structure, the strengths of the H-bond interactions between the His NH group and the PQ carbonyls are different between Q_A and Q_B as revealed by the frequency differences of the Fermi resonance peaks. The difference in the H-bonding interactions of the CO groups between Q_A and Q_B is also suggested by the slight upshift of the strongest C•••O band of semiquinone from 1478 to 1480 cm^{-1} and the changes in the feature of its satellite bands at 1470−1400 cm^{-1} (Figure 1a,c). These differences in molecular interactions of Q_A and Q_B should be related to the mechanism of fine control of their redox potentials to realize the electron flow from Q_A to Q_B. For further details of H-bond interactions of the individual carbonyls (C_1═O and C_4═O), definite assignments of the C═O stretching bands of the neutral PQ in the 1700−1600 cm^{-1} region using isotope-labeled PQ will be necessary, as has been performed in FTIR studies of bacterial Q_A and Q_B (*9*−*11*).

The Q_B^-/Q_B spectra of *Rb. sphaeroides* exhibited a positive peak at 1728 cm^{-1}, which has been proven to arise from protonation of L-Glu212 in response to Q_B^- formation (*13*−*15*). The similar positive peak at 1745 cm^{-1} (Figure 1a) in the COOH/ester C═O region of the Q_B^-/Q_B spectrum could be also caused by protonation of a carboxylate side group coupled to Q_B reduction. Because the C═O stretching band of a COOH group is known to downshift by ∼10 cm^{-1} upon deuteration (*13*−*15*, *30*), this assignment can be examined by Q_B^-/Q_B measurement in D_2O buffer.

The Q_B^-/Q_B difference spectrum of the PSII core complexes in D_2O buffer is shown in Figure 1b. Several changes were observed in this region in comparison with the spectrum in H_2O (Figure 1a). A large negative feature appeared at 1587 cm^{-1} in the amide II region, while a positive band appeared at 1465 cm^{-1} in the amide II′ (ND bend + CN stretch of deuterated amides) region. The relatively high frequency of the former feature, compared with the amide II frequency at ∼1550 cm^{-1} typical of the α-helical structure (*25*), possibly represents the specific interaction of the backbone amide around Q_B. In the amide I region, a large negative peak appeared at 1674 cm^{-1}, and the peaks at 1699, 1685, 1664, and 1657 cm^{-1} in H_2O downshifted by a few wavenumbers to 1697, 1683, 1662, and 1656 cm^{-1}, respectively, in D_2O. These changes together with the observation that the Fermi resonance peaks with a broad background (Figure 2a) due to the NH vibration disappeared in D_2O (not shown) indicate that exchangeable protons in the Q_B pocket were replaced with deuterons in D_2O buffer.

Figure 3 shows the effect of H−D exchange on the bands in the COOH/ester C═O region of the Q_B^-/Q_B and Q_A^-/Q_A spectra on an expanded scale (1770−1710 cm^{-1}). It is clearly shown that the positive peak at 1745 cm^{-1} in the Q_B^-/Q_B spectrum was unaffected by H−D exchange (Figure 3a,b). This indicates that the 1745 cm^{-1} peak is not ascribed to a COOH group. The possibility that this peak arises from an unexchangeable COOH group is unlikely, because if a carboxylate group is protonated upon Q_B^- formation, it should be involved in the proton transfer pathway like L-Glu212 in *Rb. sphaeroides*. The prominent positive peak at 1721 cm^{-1} in the Q_A^-/Q_A spectrum was also unaffected by H−D exchange (Figure 3c,d), indicative of the assignment other than a COOH group.

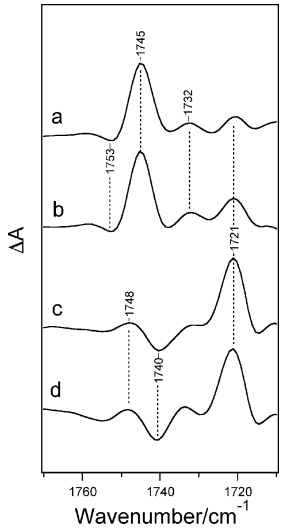

FIGURE 3: Expanded view (1770−1710 cm^{-1}) of the C═O stretching region of COOH and ester groups of the Q_B^-/Q_B and Q_A^-/Q_A FTIR difference spectra of PSII core complexes of *T. elongatus*: (a) Q_B^-/Q_B spectrum in H_2O buffer, (b) Q_B^-/Q_B spectrum in D_2O buffer, (c) Q_A^-/Q_A spectrum in H_2O buffer, and (d) Q_A^-/Q_A spectrum in D_2O buffer.

The only possible assignment other than COOH for the bands at 1750−1720 cm^{-1} in the PSII proteins is the ester C═O vibration of Chl or Pheo. The most likely assignments for the 1745 cm^{-1} peak in Q_B^-/Q_B and the 1721 cm^{-1} peak in Q_A^-/Q_A are the 10a-ester C═O stretching vibrations of adjacent $Pheo_{D2}$ and $Pheo_{D1}$, respectively. These assignments are analogous to the previous assignment of the differential signal centered at 1732 cm^{-1} in the bacterial Q_A^-/Q_A spectrum to the 10a-ester C═O group of BPheo, which was definitely determined by site-directed mutation of L-Trp100 H-bonded to this 10a-ester C═O group (*31*). According to the X-ray crystal structure of the PSII complex of *T. elongatus* (*2*), the distance from the 10a-ester C═O group of $Pheo_{D1}$ and $Pheo_{D2}$ to the Q_A and Q_B ring, respectively, is less than 9 Å. The observed shape of the 1745 and 1721 cm^{-1} bands, i.e., not a differential shape but a strong positive peak with weak negative side peaks (Figure 3), suggests that the effect of Q_A/Q_B reduction on the 10a-ester C═O vibration of $Pheo_{D1}/Pheo_{D2}$ is not merely electrostatic but through some structural coupling. The lower peak frequency by 24 cm^{-1} in Q_A^-/Q_A compared to that in Q_B^-/Q_B is consistent with the crystal structure (*2*), in which the 10a-ester C═O group of $Pheo_{D1}$ is H-bonded with D1-Tyr126, whereas the corresponding residue in the D2 subunit is D2-Phe125 that does not form a H-bond to the 10a-ester C═O group of $Pheo_{D2}$. It is noteworthy that because D1-Tyr126 is conserved in spinach, the 1721 cm^{-1} band in the Q_A^-/Q_A spectrum of *T.*

elongatus (Figure 3c) may correspond to the differential signal at 1725/1719 cm^{-1} in spinach PSII membranes, which has been temporarily assigned to the 10a-ester C═O vibration (*27*) based on the 10a-ester C═O peak at 1721 cm^{-1} in the $Pheo^-$/Pheo spectrum (*32*). Our measurement of $Pheo^-$/Pheo of *T. elongatus* core complexes also showed a negative peak at 1721 cm^{-1} (data not shown).

Not only the major peaks at 1745 and 1721 cm^{-1} but also other small peaks in this region, e.g., the peaks at 1753 and 1732 cm^{-1} in Q_B^-/Q_B (Figure 3a) and at 1748 and 1740 cm^{-1} in Q_A^-/Q_A (Figure 3c), were unaffected by H−D exchange (Figure 3b,d). This observation indicates that these small peaks also arise from ester C═O groups of Chl/Pheo or alternatively from COOH groups buried in the hydrophobic domain. It is noted that the small peak at 1721 cm^{-1} in the Q_B^-/Q_B spectrum (Figure 3a) might be ascribed to the minor contribution of the Q_A signal in the $Q_A^-Q_B \leftrightarrow Q_AQ_B^-$ equilibrium (*3*) or from centers with an unoccupied Q_B site. If this is the case, it may be estimated that ∼15% of centers stay in Q_A^-. It is also possible, however, that Q_B^-/Q_B spectrum originally has a minor band at this position.

The absence of the C═O bands of exchangeable COOH groups in the Q_B^-/Q_B spectrum indicates that protonation of carboxylate groups basically does not take place upon Q_B^- formation. This is in sharp contrast to the protonation mechanism of Q_B in *Rb. sphaeroides*, in which L-212Glu is first protonated upon Q_B^- formation (*13*−*15*). In fact, the PSII X-ray structure (*2*) showed that carboxylic amino acids are not found in the vicinity of Q_B. Instead, a number of Glu or Asp residues in the loop regions between the D and E helices of the D1 and D2 subunits (D1-Glu226, D1-Glu229, D1-Glu231, D1-Glu242, D1-Glu243, D1-Glu244, D2-Asp225, D2-Glu227, D2-Glu241, and D2-Glu242) gather in the hydrophilic domain on the stromal side of the Fe^{2+}-HCO_3^- center. Although they do not change their pK_a's in response to Q_B reduction, they could work as the entrance of the proton pathway to Q_B through bicarbonate (*7*, *33*). Another possible proton pathway is the H-bonding connection between D1-His252 on the stromal surface and D1-Ser264 H-bonded to the Q_B C═O group (*1*, *3*, *4*). Since no protonation of carboxylate residues was observed in these FTIR measurements, this His could be related to the proton uptake upon Q_B^- formation (*1*, *3*, *4*). Further studies to identify the His bands in the Q_B^-/Q_B spectrum will clarify this issue.

In conclusion, this study provides for the first time an almost pure Q_B^-/Q_B FTIR difference spectrum using the Mn-depleted PSII core complexes of *T. elongatus*. The frequencies and features of the C•••O bands of semiquinone together with the Fermi resonance peaks of the coupled His revealed the difference in H-bonding interactions between Q_A and Q_B. Spectral analysis by H−D exchange also showed that the carboxylate amino acids are not protonated upon Q_B^- formation, and thus, the protonation mechanism of Q_B in PSII is different from that in bacterial RC. Further studies using Q_B^-/Q_B measurements, combined with isotopic labeling of cofactors and proteins, and site-directed mutagenesis will provide more detailed information about the H-bond strengths of individual C═O groups of Q_B, protonation of a His side chain, the role of bicarbonate, etc. Also, the prominent signals at 1745 and 1721 cm^{-1} characteristic of the Q_B^-/Q_B and Q_A^-/Q_A spectra, respectively, which were temporarily assigned to the 10a-ester C═O groups of adjacent Pheo molecules, will be useful markers for direct detection of Q_A^- and Q_B^- in the investigation of the acceptor-side reactions. Thus, Q_B^-/Q_B FTIR measurement will be a promising tool in clarifying the molecular mechanism of the Q_B reactions in PSII.

REFERENCES

1. Diner, B. A., and Babcock, G. T. (1996) Structure, dynamics, and energy conversion efficiency in photosystm II, in *Oxygenic Photosynthesis: The Light Reactions* (Ort, D. R., and Yocum, C. F., Eds.) pp 213−247, Kluwer Academic Publishers, Dordrecht, The Netherlands.
2. Ferreira, K. N., Iverson, T. M., Maghlaoui, K., Barber, J., and Iwata, S. (2004) Architecture of the photosynthetic oxygen-evolving center, *Science 19*, 1831−1838.
3. Petrouleas, V., and Crofts, A. R. (2005) The quinone iron acceptor complex, in *Photosystem II: The Water/Plastoquinone Oxido-Reductase of Photosynthesis* (Wydrzynski, T., and Satoh, K., Eds.) Springer, Dordrecht, The Netherlands (in press).
4. Diner, B. A., Petrouleas, V., and Wendoloski, J. J. (1991) The iron-quinone electron-acceptor complex of photosystem II, *Physiol. Plant. 81*, 423−436.
5. Reifarth, F., and Renger, G. (1998) Indirect evidence for structural changes coupled with $Q_B^{-\bullet}$ formation in photosystem II, *FEBS Lett. 428*, 123−126.
6. Garbers, A., Reifarth, F., Kurreck, J., Renger, G., and Parak, F. (1998) Correlation between protein flexibility and electron transfer from $Q_A^{-\bullet}$ to Q_B in PSII membrane fragments from spinach, *Biochemistry 37*, 11399−11404.
7. van Rensen, J. J. S., Xu, C. H., and Govindjee (1999) Role of bicarbonate in photosystem II, the water-plastoquinone oxido-reductase of plant photosynthesis, *Physiol. Plant. 105*, 585−592.
8. Noguchi, T., and Berthomieu, C. (2005) Molecular analysis by vibrational spectroscopy, in *Photosystem II: The Water/Plasto-quinone Oxido-Reductase of Photosynthesis* (Wydrzynski, T., and Satoh, K., Eds.) Springer, Dordrecht, The Netherlands (in press).
9. Breton, J., Boullais, C., Berger, G., Mioskowski, C., and Nabedryk, E. (1995) Binding-sites of quinones in photosynthetic bacterial reaction centers investigated by light-induced FTIR difference spectroscopy: Symmetry of the carbonyl interactions and close equivalence of the Q_B vibrations in *Rhodobacter sphaeroides* and *Rhodopseudomonas viridis* probed by isotope labeling, *Biochemistry 34*, 11606−11616.
10. Brudler, R., de Groot, H. J. M., van Liemt, W. B. S., Gast, P., Hoff, A. J., Lugtenburg, J., and Gerwert, K. (1995) FTIR spectroscopy shows weak symmetrical hydrogen-bonding of the Q_B carbonyl groups in *Rhodobacter sphaeroides* R26 reaction centers, *FEBS Lett. 370*, 88−92.
11. Breton, J., and Nabedryk, E. (1996) Protein-quinone interactions in the bacterial photosynthetic reaction center: Light-induced FTIR difference spectroscopy of the quinone vibrations, *Biochim. Biophys. Acta 1275*, 84−90.
12. Okamura, M. Y., Paddock, M. L., Graige, M. S., and Feher, G. (2000) Proton and electron transfer in bacterial reaction centers, *Biochim. Biophys. Acta 1458*, 148−163.
13. Hienerwadel, R., Grzybek, S., Fogel, C., Kreutz, W., Okamura, M. Y., Paddock, M. L., Breton, J., Nabedryk, E., and Mäntele, W. (1995) Protonation of Glu-L212 following Q_B^- formation in the photosynthetic reaction center of *Rhodobacter sphaeroides*: Evidence from time-resolved infrared spectroscopy, *Biochemistry 34*, 2832−2843.
14. Nabedryk, E., Breton, J., Hienerwadel, R., Fogel, C., Mäntele, W., Paddock, M. L., and Okamura, M. Y. (1995) Fourier-transform infrared difference spectroscopy of secondary quinone acceptor photoreduction in proton-transfer mutants of *Rhodobacter sphaeroides*, *Biochemistry 34*, 14722−14732.
15. Nabedryk, E., Breton, J., Okamura, M. Y., and Paddock, M. L. (2004) Identification of a novel protonation pattern for carboxylic acids upon Q_B photoreduction in *Rhodobacter sphaeroides* reaction center mutants at Asp-L213 and Glu-L212 sites, *Biochemistry 43*, 7236−7243.
16. Breton, J., Boullais, C., Mioskowski, C., Sebban, P., Baciou, L., and Nabedryk, E. (2002) Vibrational spectroscopy favors a unique Q_B binding site at the proximal position in wild-type reaction centers and in the Pro-L209 → Tyr mutant from *Rhodobacter sphaeroides*, *Biochemistry 41*, 12921−12927.

17. Nabedryk, E., Breton, J., Sebban, P., and Baciou, L. (2003) Quinone (Q_B) binding site and protein stuctural changes in photosynthetic reaction center mutants at Pro-L209 revealed by vibrational spectroscopy, *Biochemistry 42*, 5819−5827.
18. Breton, J. (2004) Absence of large-scale displacement of quinone Q_B in bacterial photosynthetic reaction centers, *Biochemistry 43*, 3318−3326.
19. Stowell, M. H. B., McPhillips, T. M., Rees, D. C., Soltis, S. M., Abresch, E., and Feher, G. (1997) Light-induced structural changes in photosynthetic reaction center: Implications for mechanism of electron-proton transfer, *Science 276*, 812−816.
20. Zhang, H., Fischer, G., and Wydrzynski, T. (1998) Room-temperature vibrational difference spectrum for $S_2Q_B^-/S_1Q_B$ of photosystem II determined by time-resolved Fourier transform infrared spectroscopy, *Biochemistry 37*, 5511−5517.
21. Sugiura, M., and Inoue, Y. (1999) Highly purified thermo-stable oxygen-evolving photosystem II core complex from the thermophilic cyanobacterium *Synechococcus elongatus* having His-tagged CP43, *Plant Cell Physiol. 40*, 1219−1231.
22. Noguchi, T., and Sugiura, M. (2002) Flash-induced FTIR difference spectra of the water oxidizing complex in moderately hydrated photosystem II core films: Effect of hydration extent on S-state transitions, *Biochemistry 41*, 2322−2330.
23. Bauscher, M., Nabedryk, E., Bagley, K., Breton, J., and Mäntele, W. (1990) Investigation of models for photosynthetic electron acceptors. Infrared spectroelectrochemistry of ubiquinone and its anions, *FEBS Lett. 261*, 191−195.
24. Socrates, G. (1994) *Infrared Characteristic Group Frequencies*, pp 90−102, John Wiley & Sons, Chichester, U.K.
25. Venyaminov, S. Yu., and Kalnin, N. N. (1990) Quantitative IR spectrophotometry of peptide compounds in water (H_2O) solutions. II. Amide absorption bands of polypeptides and fibrous proteins in α-, *β*-, and random coil conformations, *Biopolymers 30*, 1259−1271.
26. Remy, A., Niklas, J., Kuhl, H., Kellers, P., Schott, T., Rögner, M., and Gerwert, K. (2004) FTIR spectroscopy shows structural similarities between photosystems II from cyanobacteria and spinach, *Eur. J. Biochem. 271*, 563−567.
27. Berthomieu, C., Nabedryk, E., Mäntele, W., and Breton, J. (1990) Characterization by FTIR spectroscopy of the photoreduction of the primary quinone acceptor Q_A in photosystem II, *FEBS Lett. 269*, 363−367.
28. Noguchi, T., Inoue, Y., and Tang, X. S. (1999) Hydrogen bonding interaction between the primary quinone acceptor Q_A and a histidine side chain in photosystem II as revealed by Fourier transform infrared spectroscopy, *Biochemistry 38*, 399−403.
29. Breton, J., and Nabedryk, E. (1998) Proton uptake upon quinone reduction in bacterial reaction centers: IR signature and possible participation of a highly polarizable hydrogen bond network, *Photosynth. Res. 55*, 301−307.
30. Siebert, F., Mäntele, W., and Kreutz, W. (1982) Evidence for the protonation of two internal carboxylic groups during the photocycle of bacteriorhodopsin. Investigation by kinetic infrared spectroscopy, *FEBS Lett. 141*, 82−87.
31. Breton, J., Nabedryk, E., Allen, J. P., and Williams, J. C. (1997) Electrostatic influence of Q_A reduction on the IR vibrational mode of the 10a-ester C═O of H_A demonstrated by mutations at residues Glu L104 and Trp L100 in reaction centers from *Rhodobacter sphaeroides*, *Biochemistry 36*, 4515−4525.
32. Nabedryk, E., Andrianambinintsoa, S., Berger, G., Leonhard, M., Mäntele, W., and Breton, J. (1990) Characterization of bonding interactions of the intermediary electron acceptor in the reaction center of Photosystem II, *Biochim. Biophys. Acta 1016*, 49−54.
33. Berthomieu, C., and Hienerwadel, R. (2001) Iron coordination in photosystem II: Interaction between bicarbonate and the Q_B pocket studied by Fourier transform infrared spectroscopy, *Biochemistry 40*, 4044−4052.

BI051237G